General

Protected amino acids, resins, building blocks and coupling reagents for peptide synthesis were obtained from NovaBiochem, tBu$_2$SiF$_2$ was purchased from ABCR and all other chemicals were obtained from SigmaAldrich in highest available grade and used without further purification. ^{18}F was obtained from the Department of Nuclear Medicine Rechts der Isar (Munich), MBIC (Montreal), ZAG (Eggenstein-Leopoldshafen) and EuroPET AG (Freiburg), the used ^{68}Ge/^{68}Ga-Generator (Obninsk type) was obtained from Eckert & Ziegler Eurotope GmbH and ^{177}Lu was obtained from ITG GmbH (Garching). The NMR experiments were performed with a JNM-Eclipse 400. The chemical shifts (δ) are given in ppm and tetramethylsilane (TMS) was used as reference. Mass spectra were obtained using either matrix-assisted laser desorption/ionization (Bruker Microflex), electron ionization (Hewlett Packard 5989 A Mass Spectrometer with 59980 B Particle Beam LC/MS Interface) or electron spray ionization (Jeol JMS GCmate II). Reaction control and quality control analyses were carried out using either an Agilent 1200 series or a Dionex UltiMate 3000 HPLC system equipped with a Gabi-Star (Raytest) radioactivity detector. With both systems, a Chromolith Performance RP18e column (100 x 4.6 mm, Merck) was used as stationary phase (mobile phase: gradient 0-100 % H_2O to acetonitrile + 0.1 % TFA, 4 mL/ min, 5 min).

Synthesis of peptides by solid phase peptide synthesis (SPPS)

SiFA- and SiFA*lin*-derivatized somatostatin-analogs were synthesized as described earlier (*1*, *2*). In brief, the Tyr^3-octreotate was synthesized and derivatized at the *N*-terminus by introduction of hydrophilic auxiliaries (Fmoc-NH-PEG$_n$-COOH (n = 1, 2, 3, 5,

27), Fmoc-Asp(OtBu)-OH, Fmoc-Asn(Ac_3AcNH-β-Glc)-OH, and Boc_2-Aoa-OH) using standard Fmoc solid-phase peptide synthesis protocols. After cleavage of the peptides from the resin under acidic conditions, the crude peptides were purified using semipreparative HPLC. The cleavage of the carbohydrate-acetyl protecting groups was carried out using sodium methanolate in methanol. The re-purified peptides were incubated with an excess of the corresponding SiFA-synthon (either SiFA-aldehyde or freshly prepared SiFA*lin*-aldehyde) in phosphate buffer at pH 4.0 to obtain the SiFA- and SiFA*lin*-conjugated products. When conjugating SiFA*lin*-aldehyde, the freshly prepared SiFA*lin*-aldehyde was dissolved in a 1:1 mixture of phosphate buffer (pH 4.0) and acetonitrile and the pH was adjusted to pH 4.0 with 5 - 10 µL 4N sodium hydroxide solution. Subsequently, the peptides were purified using semipreparative HPLC and isolated as white solids after lyophilization.

Analytical data for peptides **4**-**13**:

4: MALDI (m/z): for $[M+H]^+$ (calculated): 2,065.0 (2,063.3).

5: MALDI (m/z): for $[M+2H]^{2+}$ (calculated): 2,123.8 (2,121.4).

6: MALDI (m/z): for $[M+H]^+$ (calculated): 2,166.2 (2,165.4).

7: MALDI (m/z): for $[M+H]^+$ (calculated): 2,254.3 (2,253.6).

8: MALDI (m/z): for $[M+2H]^{2+}$ (calculated): 3,109.5 (3,107.6).

9: MALDI (m/z): for $[M+H]^+$ (calculated): 2,162.9 (2,161.9).

10: MALDI (m/z): for $[M+H]^+$ (calculated): 2,221.0 (2,220.0).

11: MALDI (m/z): for $[M+H]^+$ (calculated): 2,265.0 (2,264.0).

12: MALDI (m/z): for $[M+H]^+$ (calculated): 2,353.4 (2,352.1).

13: MALDI (m/z): for $[M+2H]^{2+}$ (calculated): 3,207.9 (3,205.6).

Preparation of SiFA and SiFA*in* aldehyde for peptide conjugation

The preparation of the intermediates 4-[tert-butyldimethylsiloxy)-methyl]phenyl bromide (**14**)(*3*), Di-tert-butyl{4-[tert-butyldimethylsiloxy)methyl]phenyl}fluorosilane (**15**)(*4*), (4-(di-tert-butylfluorosilyl)phenyl)methanol (**16**)(*4*), (4-(bromomethyl)phenyl)di-tert-butylfluorosilane (**18**)(*5*), and the SiFA-aldehyde (4-(Di-tert-butylfluorosilyl)benzylaldehyde, **17**)(*4*) was carried out according to published protocols.

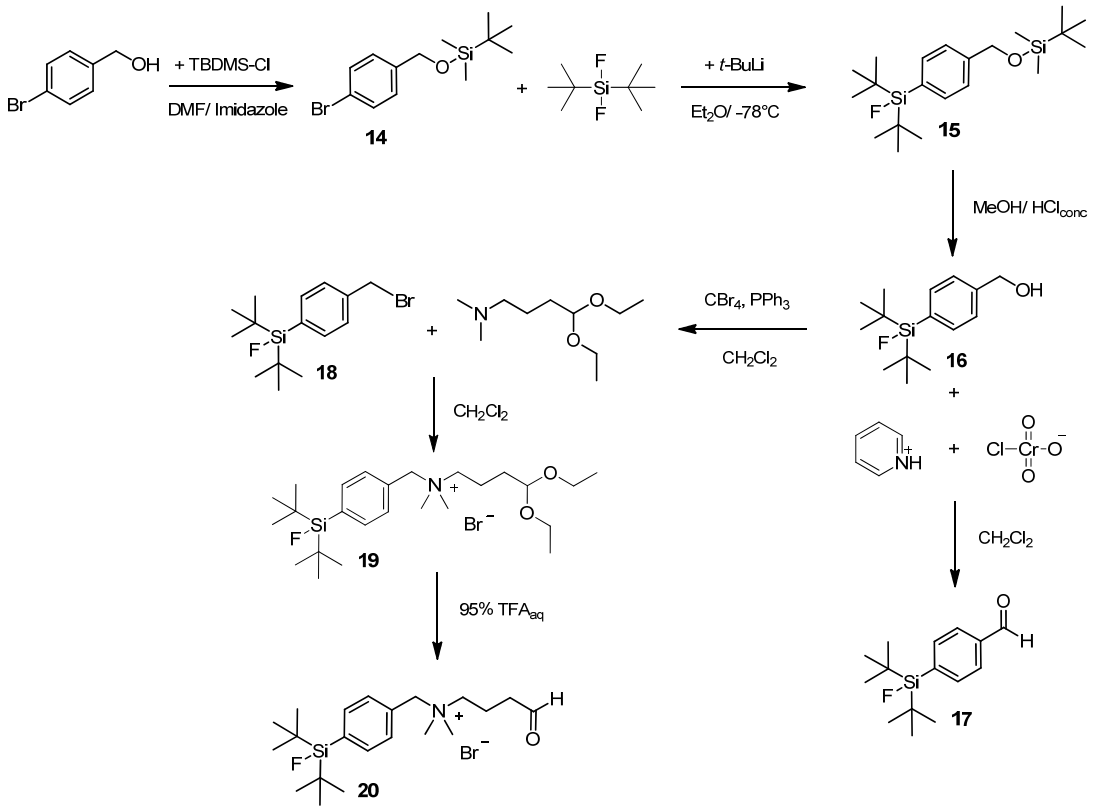

Supplemental Scheme 1: Schematic depiction the synthesis of SiFA and SiFA*in* aldehydes used for the conjugation to hydrophilic peptide cores.

Synthesis of N-(4-(di-tert-butylfluorosilyl)benzyl)-4,4-diethoxy-N,N-dimethylbutan-1-ammonium bromide (**19**):

To a solution of 1.2 g (3.5 mmol) (4-(bromomethyl)phenyl)di-tert-butylfluorosilane (**18**) in 100 mL anhydrous dichloromethane (CH_2Cl_2) a solution containing 4-(dimethylamino)butanal diethyl acetal (359.1 mg, 3.5 mmol) in 25 mL anhydrous CH_2Cl_2 was added and stirred at ambient temperature overnight. Subsequently, the solvent was evaporated *in vacuo* to give **19** as white solid (1.8 g, 99%).

Analytical data for **19**:

^{1}H-NMR (400 MHz, Aceton-d_6) δ 7.92 (d, J=8.0 Hz, 2H; H_o), 7.75 (d, J=8,0 Hz, 2H; H_m), 5.18 (s, 2H; N-CH_2-aromatic), 4.63 (t, J=5.3 Hz, 1H; CH), 3.82-3.74 (m, 2H; N-CH_2), 3.66-3.58 (m, 2H; O-CH_2), 3.54-3.46 (m, 2H; O-CH_2), 3.35 (s, 6H; N-CH_3), 2.05-2.03 (m, 2H; CH_2-C*H*$_2$-CH_2), 1.69-1.66 (m, 2H; CH_2-C*H*$_2$-CH), 1.12 (t, 6H; CH_2-C*H*$_3$), 1.06 (s, 18H; CH_3).

^{13}C-NMR (101 MHz, Aceton-d_6) δ 136.02 (d, J (^{13}C, ^{19}F)=13.8 Hz; C_p), 134.28 (d, J (^{13}C, ^{19}F)=4.3 Hz; C_m), 132.73 (d, J (^{13}C, ^{19}F)=1.0 Hz; C_o), 101.91 (s; CH), 66.03 (s; N-*C*H_2-aromatic), 63.56 (s; N-CH_2), 61.24 (s; O-CH_2), 61.21 (s; O-CH_2), 49.08 (s; N-CH_3), 30.41 (s; CH-*C*H_2), 26.79 (s; *tert*-butyl-CH_3), 19.90 (d, J (^{13}C, ^{19}F)=12.3 Hz; Si-CH_2),17.89 (s; CH_2-*C*H_2-CH_2), 14.99 (s; CH_2-*C*H_3).

EI-MS (m/z) for $[M + H]^+$ (calculated): 440.3 (440.7).

Synthesis of N-(4-(di-tert-butylfluorosilyl)benzyl)-N,N-dimethyl-4-oxobutan-1-ammonium bromide (**20**):

To 10.0 mg (19.2 µmol) **19** were added 100 µL 95 % TFA in H_2O and the reaction was left to stand without stirring at ambient temperature for 30 min. The reaction was quenched with the addition of anhydrous diethylether (Et_2O) (1.5 mL) and cooled to -20°C overnight. The appearing white precipitate was fixed by centrifugation (5 min at

14,100 x g) and the supernatant was decanted. The resulting pellet was used immediately in the subsequent reaction without further purification or evaporation.

Analytical data for **20**:

ESI-MS (m/z) for $[M + H]^+$ (calculated): 366.3 (366.3).

Cell culture

AR42J cells were purchased from European Collection of Cell Cultures (ECACC No. 93100618) and incubated using RPMI 1640 medium supplemented with 20% FCS and 2 mM glutamine at 37°C in humidified air, equilibrated with 5 % CO_2 according to HPA cultures recommendations. Harvesting of the cells grown at 70-80% confluence was carried out using 0.05% trypsin/EDTA, separating cell clusters was performed using a 40 µm cell strainer and cell resuspension after centrifugation either in binding buffer for in vitro testing or RPMI 1640 medium without supplements for tumor inoculation.

AR42J xenograft mouse model

All animal experiments were performed according to the German animal protection laws and protocols of the local committee. 100 µL of cell suspension containing 5 x 10^6 AR42J cells were inoculated subcutaneously into the left flank of 7-9 weeks old female nude mice (CD1-*Foxn1*^{nu}, Charles River). Mice demonstrating palpable tumors of approximately 0.2 - 0.8 cm^3 at 10 - 17 days after tumor inoculation were used for biodistribution or PET imaging experiments.

Preparation of ^{68}Ga-DOTATATE and ^{177}Lu-DOTATATE

Preparation of ^{68}Ga-DOTATATE. 25 µL of an aqueous stock solution (1 mM) containing DOTATATE were added to 1.2 mL $^{68}GaCl_3$ (pH adjusted to 3.75 with 1,25 M NaOAc), heated to 99° C for 10 min and cooled before purifying the crude product using a SepPak C18 cartridge. The radiolabeled peptide was eluted with ethanol in 100-200µL fractions. The aliquot containing the highest activity was prepared for injection by addition of water for injection to obtain an ethanol proportion of ≤10%. The product was ≥99% pure as confirmed by analytical radio-HPLC.

Preparation of ^{177}Lu-DOTATATE. 7.2 - 7.8 GBq (194 - 210 mCi) $^{177}LuCl_3$ in 0.1 - 0.4 mL 0.04 M HCl were added to a solution containing 250 µg DOTATATE, 0.2 M acetate-buffer (pH 4.8) and 0.052 - 0.065 gentisic acid and heated to 100° C for 30 min. After cooling to ambient temperature, 8 - 9 mL water for injection were added and the product was filtered for sterility. The product was ≥99% pure as confirmed by analytical radio-HPLC.

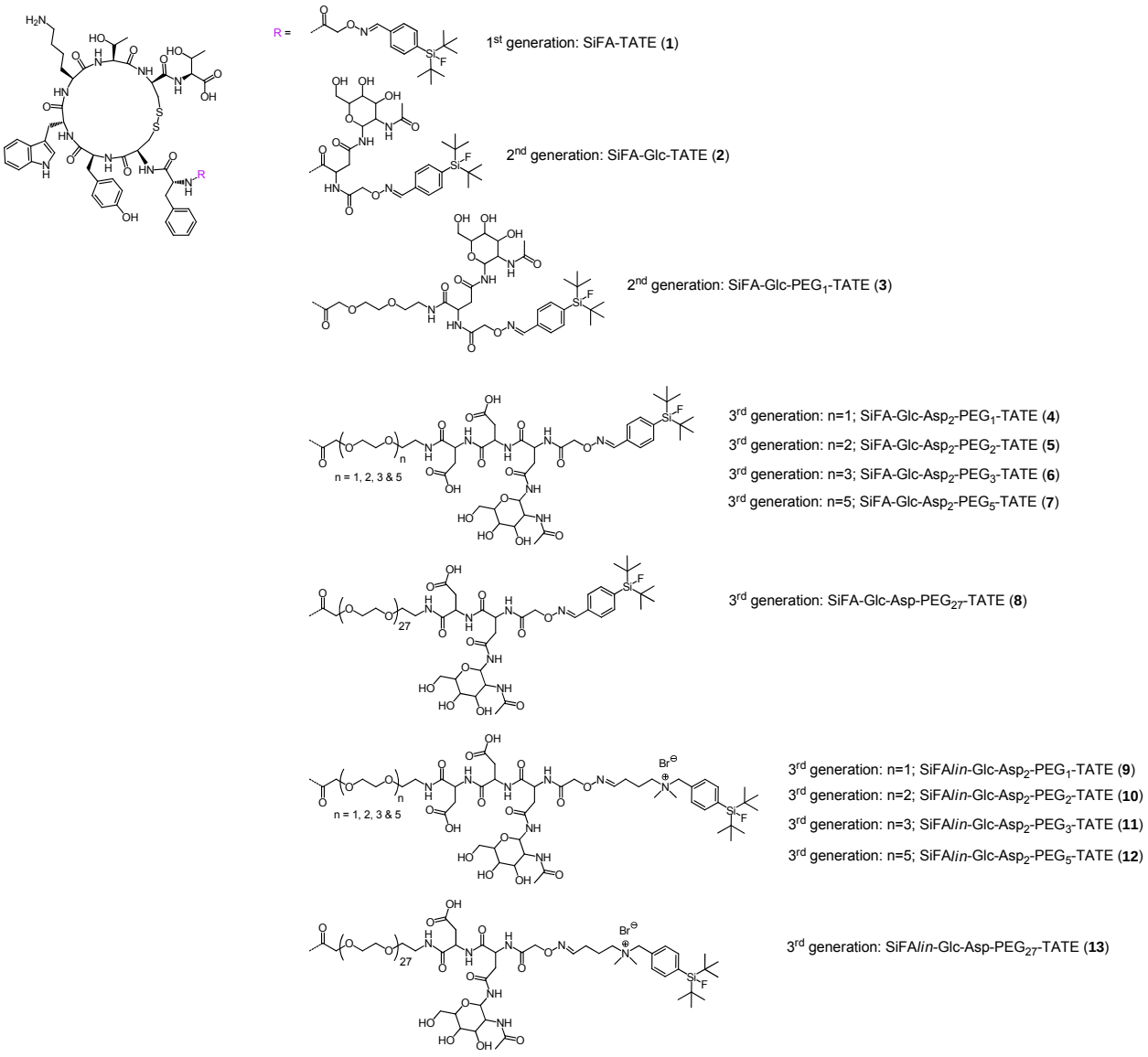

Supplemental Figure 1: Structures of 1st, 2nd, and 3rd generation SiFA-derivatized somatostatin-analogs **1** - **13**. The 1st generation analog SiFA-TATE does not comprise any hydrophilic auxiliaries as the SiFA moiety is directly conjugated to the peptide. The 2nd generation peptide derivatives **2** and **3** comprise a carbohydrate and PEG_1 auxiliary in order to obtain SiFA-TATE-derivatives of higher hydrophilicity. Finally, the 3rd generation derivatives **4** - **13** were systematically varied with carbohydrate, PEG linkers, aspartic acids and different SiFA building blocks (either SiFA or SiFa*lin*) in order to evaluate the most

promising compound regarding in vivo tumor imaging and pharmacokinetic properties.

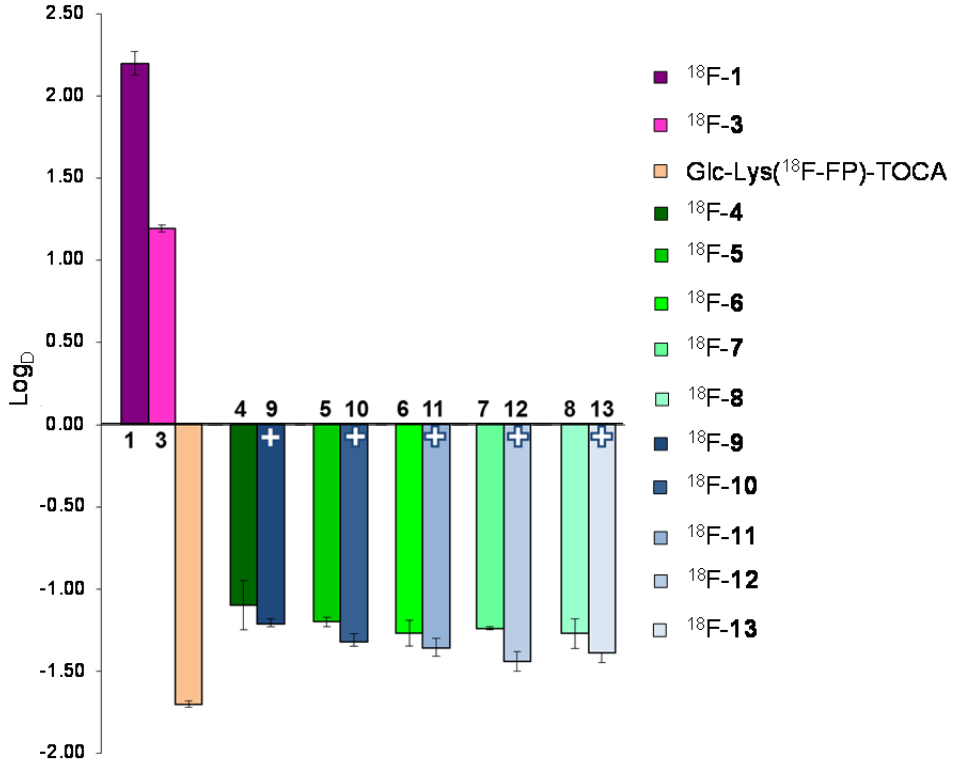

Supplemental Figure 2: The introduction of additional hydrophilic auxiliaries decreases the overall lipophilicity of 3rd generation SiFA- and SiFA*lin*-TATEs substantially compared to 1st and 2nd generation SiFA-TATE derivatives. Log_D values (n-octanol/phosphate buffer (pH 7.4) partition coefficients) of 3rd generation SiFA (green) and SiFA*lin* (blue) derivatized somatostatin analogs **4** - **13** were evaluated using the shake-flask method (sample measurement n = 3, error bars represent means ± s.d.). As a reference, the values for the 1st (purple) and 2nd (magenta) generation SiFA-Tyr^3-octreotate derivatives **1** and **3** as well as a non-SiFA-derivatized ^{18}F-labeled somatostatin analog Glc-Lys([^{18}F]FP)-TOCA are given (*6*, *7*).

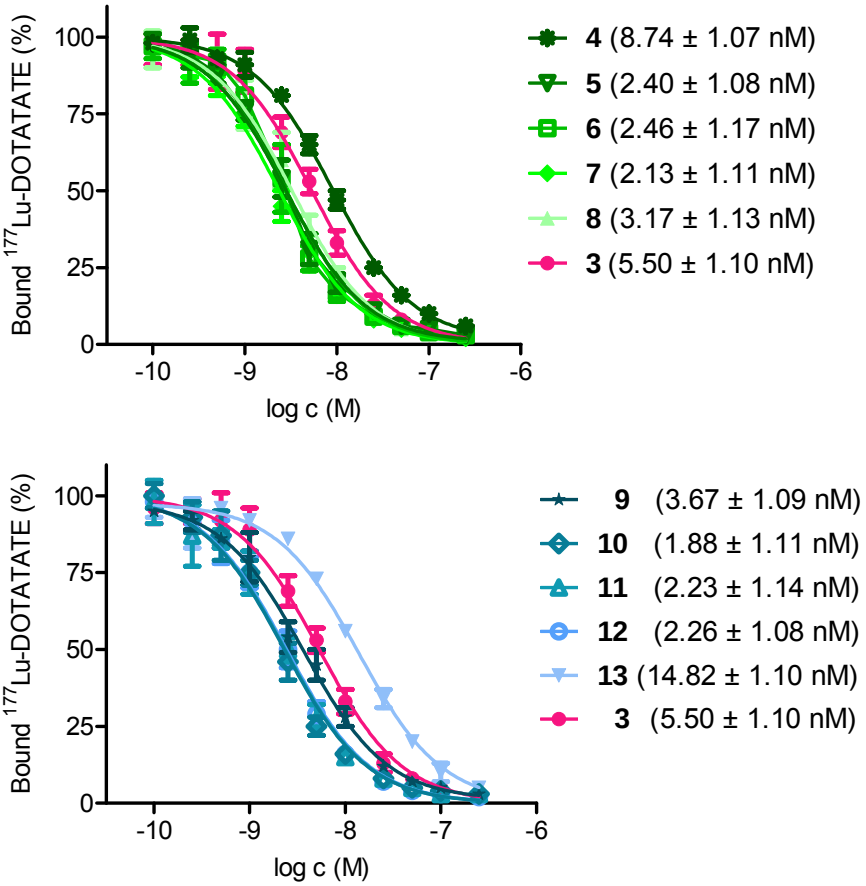

Supplemental Figure 3: High tolerance of Tyr^3-octreotate to hydrophilic chemical modifications without loss of bioactive potency. Binding affinities of 3rd generation SiFA- (green) and SiFA*lin*- (blue) derivatized somatostatin-analogs compared to 2nd generation **3** (magenta) were evaluated by competitive receptor affinity studies using viable AR42J cells and ^{177}Lu-DOTATATE as competitor. After incubation for 60 min in binding buffer at ambient temperature and successive washing steps the cell-bound activity was measured using a gamma counter. All experiments were performed thrice separately (error bars represent means ± s.d.).

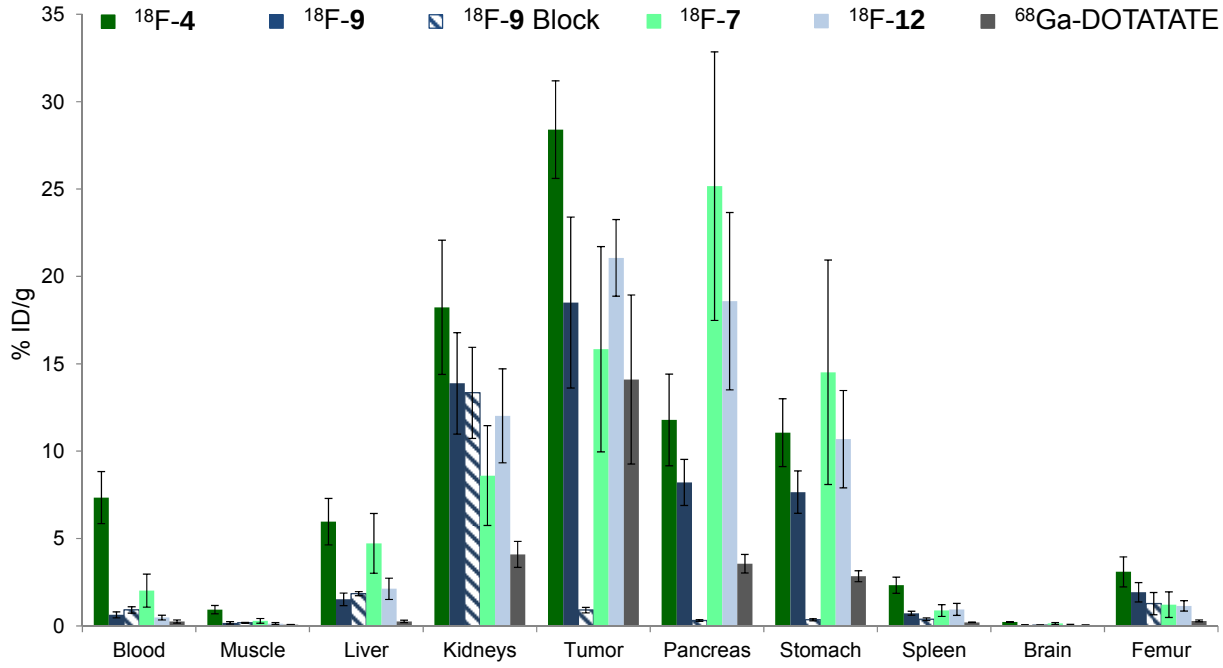

Supplemental Figure 4: Despite an exceedingly high tumor accumulation of ^{18}F-**4** the SiFA*lin*-derivatized counterpart ^{18}F-**9** shows a more favorable distribution and excretion in vivo. Results from the ex vivo biodistribution studies of the 3rd generation ^{18}F-SiFA-TATE derivatives ^{18}F-**4** (n = 5), ^{18}F-**9** (n = 10), ^{18}F-**7** (n = 5), and ^{18}F-**12** (n = 4) and the clinical gold standard ^{68}Ga-DOTATATE (n = 5) obtained from AR42J tumor-bearing xenograft mice at 60 min p.i. The values are given as % ID/g for each organ (error bars represent means ± s.d.). For the most promising newly developed radiotracer ^{18}F-**9**, a blocking experiment using 200 µg/mouse DOTATATE (n = 5) was performed (dashed blue columns), showing the specific binding to the SSTR-bearing tumor and physiologic SSTR-positive tissues.

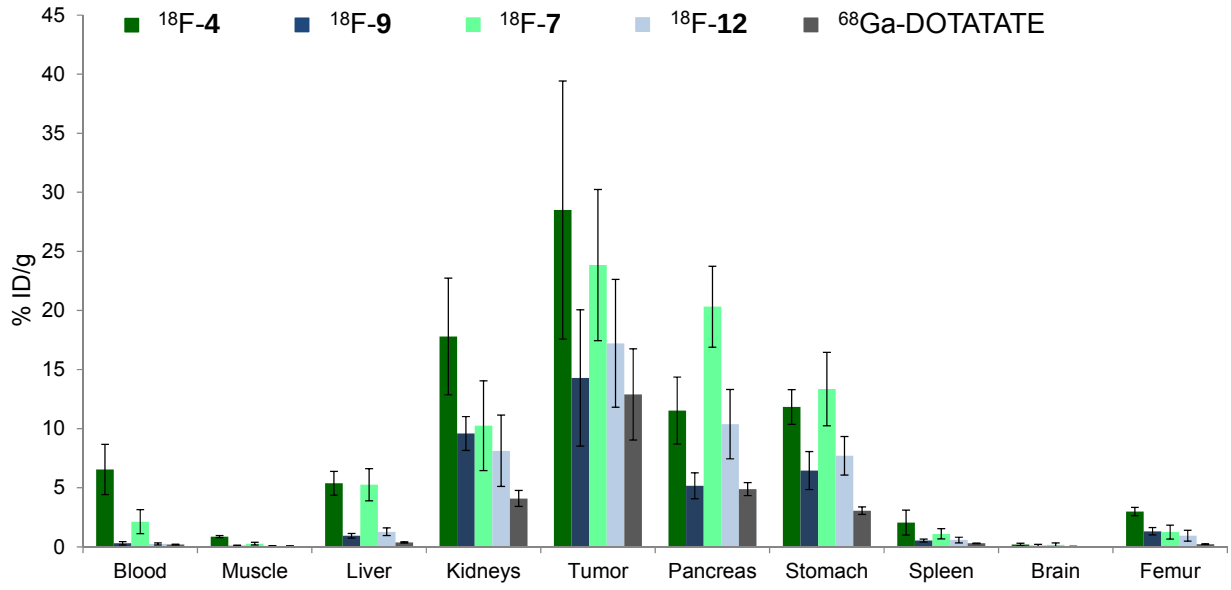

Supplemental Figure 5: At 90 min p.i. the ^{18}F-SiFA*lin*-derivatized somatostatin-analog ^{18}F-**9** demonstrates the same favorable in vivo activity accumulation as the gold standard ^{68}Ga-DOTATATE. Results from the ex vivo biodistribution studies of the 3rd generation ^{18}F-SiFA-TATE derivatives ^{18}F-**4** (n = 3), ^{18}F-**9** (n = 10), ^{18}F-**7** (n = 5), and ^{18}F-**12** (n = 5) compared to the gold standard ^{68}Ga-DOTATATE (n = 5) in various tissues at 90 min p.i. The values are given as % ID/g for each organ (error bars represent means ± s.d.).

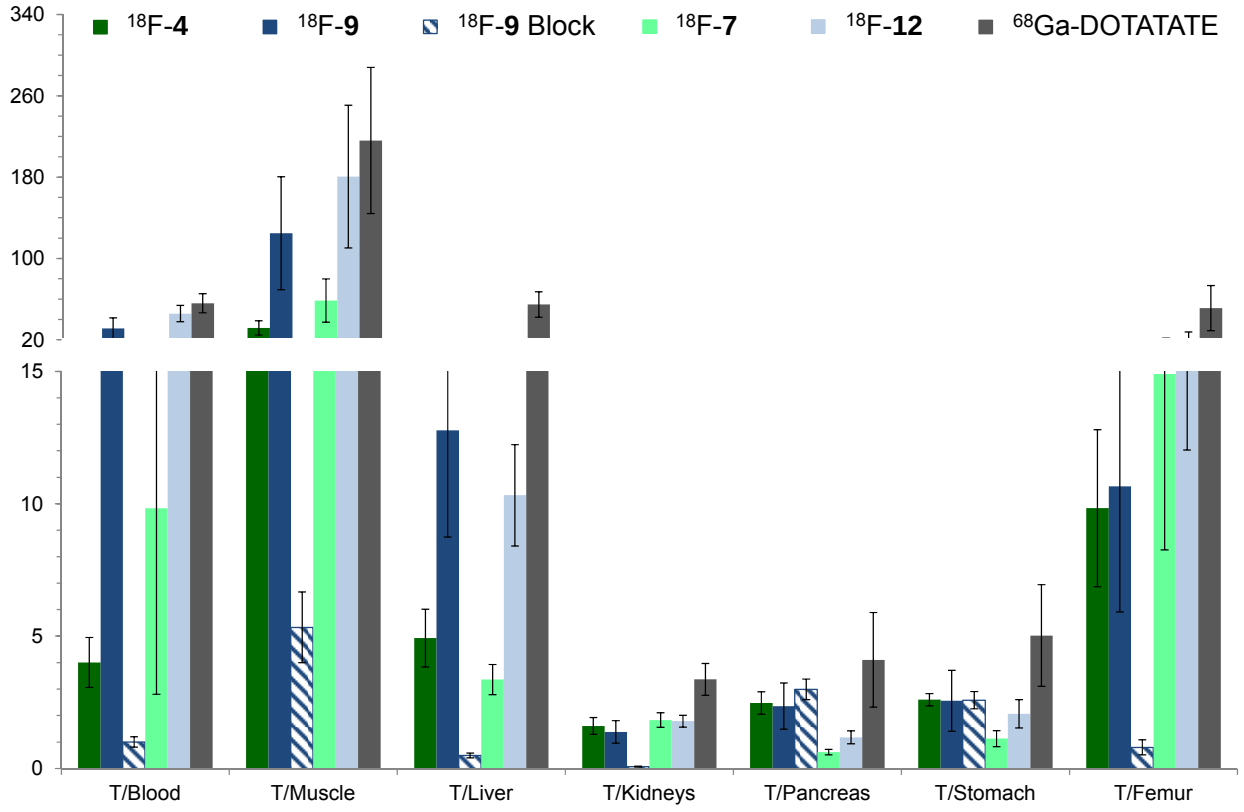

Supplemental Figure 6: ^{18}F-SiFA*lin*-building block-derivatized somatostatin-analogs enable tumor-to-background ratios comparable to the gold standard ^{68}Ga-DOTATATE. Tumor-to-organ ratios of selected organs obtained from the ex vivo biodistribution experiments of the 3rd generation ^{18}F-SiFA- and SiFA*lin*-TATE derivatives ^{18}F-**4** (n = 5), ^{18}F-**9** (n = 10), ^{18}F-**7** (n = 5), and ^{18}F-**12** (n = 4) and the clinical gold standard ^{68}Ga-DOTATATE (n = 5) in AR42J tumor-bearing xenograft mice at 60 min p.i. The values are given as % ID/g for each organ (error bars represent means ± s.d.). For ^{18}F-**9**, a blocking experiment (n = 5) using 200 µg/mouse DOTATATE was performed (dashed blue columns), showing the specific binding to the SSTR-bearing tumor and physiologic SSTR-positive tissues. These results display the SiFA*lin*-building block-derivatized somatostatin-analogs to feature higher tumor-to-organ ratios than their uncharged SiFA counterparts.

REFERENCES

1. Wängler C, Waser B, Alke A, et al. One-Step F-18-labeling of carbohydrate-conjugated octreotate-derivatives containing a Silicon-Fluoride-Acceptor (SiFA): In vitro and in vivo evaluation as tumor imaging agents for Positron Emission Tomography (PET). *Bioconj Chem.* 2010;21:2289-2296.
2. Wängler C, Niedermoser S, Chin JS, et al. One-step F-18-labeling of peptides for positron emission tomography imaging using the SiFA methodology. *Nat Protoc.* 2012;7:1946-1955.
3. Corey E, Venkateswarlu A. Protection of hydroxyl groups as tert-butyldimethylsilyl derivatives. *J Am Chem Soc.* 1972;94:6190-6191.
4. Iovkova L, Wängler B, Schirrmacher E, et al. para-Functionalized aryl-di-tert-butylfluorosilanes as potential labeling synthons for 18F radiopharmaceuticals. *Chem-Eur J.* 2009;15:2140-2147.
5. Kostikov AP, Iovkova L, Chin J, et al. N-(4-(di-tert-butyl[F-18]fluorosilyl)benzyl)-2-hydroxy-N,N-dimethylethylammonium bromide ([F-18]SiFAN(+)Br(-)): A novel lead compound for the development of hydrophilic SiFA-based prosthetic groups for F-18-labeling. *J Fluorine Chem.* 2011;132:27-34.
6. Meisetschlager G, Poethko T, Stahl A, et al. Gluc-Lys([F-18]FP)-TOCA PET in patients with SSTR-positive tumors: Biodistribution and diagnostic evaluation compared with [In-111]DTPA-octreotide. *J Nucl Med.* 2006;47:566-573.
7. Wieder H, Beer AJ, Poethko T, et al. PET/CT with Gluc-Lys-([F-18]FP)-TOCA: correlation between uptake, size and arterial perfusion in somatostatin receptor positive lesions. *Eur J Nucl Med Mol Imaging.* 2008;35:264-271.